UCRL-JRNL-204740

Simulations of present and future climates in the western U.S. with four nested regional climate models

P. B. Duffy[1], R. W. Arritt[2], J. Coquard[1], W. Gutowski[2], J. Han[3], J. Iorio[1], J. Kim[4], L-R Leung[5], J. Roads[6], E. Zeledon[1]

[1]Lawrence Livermore National Laboratory
[2]Iowa State University
[3]National Centers for Environmental Prediction
[4]University of California, Los Angeles
[5]Pacific Northwest National Laboratory
[6]University of California, San Diego

This paper was submitted to: Journal of Climate

June/2004

UCRL-JRNL-204740

Simulations of present and future climates in the western U.S. with four nested regional climate models

P. B. Duffy[1], R. W. Arritt[2], J. Coquard[1], W. Gutowski[2], J. Han[3], J. Iorio[1], J. Kim[4], L-R Leung[5], J. Roads[6], E. Zeledon[1]

[1]Lawrence Livermore National Laboratory

[2]Iowa State University

[3]National Centers for Environmental Prediction

[4]University of California, Los Angeles

[5]Pacific Northwest National Laboratory

[6]University of California, San Diego

Abstract

We analyze simulations of present and future climates in the western U.S. performed with four regional climate models (RCMs) nested within two global ocean-atmosphere climate models. Our primary goal is to assess the range of regional climate responses to increased greenhouse gases in available RCM simulations. The four RCMs used different geographical domains, different increased greenhouse gas scenarios for future-climate simulations, and (in some cases) different lateral boundary conditions. For simulations of the present climate, we compare RCM results to observations and to results of the GCM that provided lateral boundary conditions to the RCM. For future-climate (increased greenhouse gas) simulations, we compare RCM results to each other and to results of the driving GCMs. When results are spatially averaged over the western U.S., we find that the results of each RCM closely follow those of the driving GCM in the same region, in both present and future climates. In present-climate simulations, the RCMs have biases in spatially-averaged simulated precipitation and near-surface temperature that seem to be very close to those of the driving GCMs. In future-climate simulations, the spatially-averaged RCM-projected responses in precipitation and near-surface temperature are also very close to those of the respective driving GCMs. Precipitation responses predicted by the RCMs are in many regions not statistically significant compared to interannual variability. Where the predicted precipitation responses are statistically significant, they are positive. The models agree that near-surface temperatures will increase, but do not agree on the spatial pattern of this increase. The four RCMs produce very different estimates of water content of snow in the present climate, and of the change in this water content in response to increased greenhouse gases.

1. Introduction

Accurate projections of future regional-scale climates are needed to assess the possible societal impacts of climate change. These impacts may include effects on water availability, agriculture, human health, and so on. Uncertainties in projections of regional-scale climate change complicate the process of assessing societal impacts and of making policy decisions to cope with climate change. Systematic studies are needed to quantify uncertainties in regional climate changes, to identify the sources of those uncertainties, and ultimately to reduce them.

In this paper we start evaluating uncertainties in future climate in the Western U.S. by intercomparing simulations of this region performed with four regional climate models (RCMs) nested within two different global climate models (GCMs). Our goals are to assess (1) how well the different RCM/GCM combinations simulate aspects of the present climate in this region; and (2) the inter-model range of projected regional climate responses to increased atmospheric greenhouse gases. Because we are particularly interested in the possible impacts of climate change on water availability, we focus on meteorological variables relevant to this problem: near-surface temperatures, precipitation, and water-equivalent snow depth. We emphasize that errors in the RCM results are not necessarily due to problems in the RCM itself, but may instead reflect errors in the GCM-based lateral boundary conditions. Thus in our analyses of present-

climate simulations we are not evaluating the RCMs per se but rather the coupled RCM/GCM models.

Our approach has some significant limitations. First, the RCM simulations we analyzed use different spatial resolutions, different geographical domains, different increased greenhouse gas scenarios for future-climate simulations, and (in some cases) different lateral boundary conditions. Thus, this is not a formal model intercomparison study, but rather an attempt to learn from available simulations. Several carefully-controlled studies—the U.S. Project to Intercompare Regional Climate Simulations (PIRCS; Takle *et al.,* 1999); the Euopean Prediction of Regional Scenarios and Uncertainties for Defining European Climate Change Risks and Effects (PRUDENCE; Christensen *et al.* 2002) project, the Canadian Climate Impacts Scenarios (CCIS, 2004) project, and the Regional Model Intercomparison Project (RMIP, 2003) for Asia—are under way, however. Second, it is important to avoid equating future-climate uncertainties to inter-model differences. There are important uncertainties (notably in future greenhouse gas levels and other climate perturbations) that are external to climate models. Also, of course, there may be important errors common to all the models we look at. For these reasons, inter-model differences in projected future climates may be much smaller than actual uncertainties in future climate. I.e., the true future climate may be outside the envelope of model projections. Finally, the approach of evaluating future-climate uncertainties by assessing inter-model differences implicitly assumes that all models are equally credible. In principle, models that do a better job of simulating the present climate should give more credible projections than other models do. One attempt to

narrow future-climate uncertainties by eliminating models that are relatively unskilled at simulating the present climate was not successful, however (Coquard et al, 2004).

It should also be noted that RCMs cannot be expected to accurately reproduce observations of the present climate if they are driven by boundary data which contains significant biases. Thus the best test of the RCM dynamics and parameterized physics is to drive the model with reanalysis (i.e. with the best possible boundary conditions). When driving an RCM with present-climate data from a free-running global climate model, the best one can expect from the RCM is accurate downscaling of the GCM solution (biases and all). Also, the GCMs that provided lateral boundary conditions were free-running models that computed ocean temperatures, salinity and circulation internally. A further step in the comparison would be to use boundary conditions from GCMs that simulated present climate with prescribed, observed sea-surface temperatures (SSTs). The analysis here is thus one part of a broader analysis that could also include RCMs driven by reanalyses and RCMs driven by GCMs with specified SSTs.

2. Description of models, simulations, and observations

We analyzed simulations of present and future climates performed with four different RCMs. These RCM simulations were all driven by lateral boundary conditions from global ocean-atmosphere general circulation models (GCMs). The simulations with the PNNL and ECPC RCMs were both driven by results from the NCAR DOE Parallel Climate model (PCM); however different PCM simulations were used for the PNNL vs.

ECPC simulations. The UCLA and Iowa State simulations were both driven by the same simulations performed with the HadCM2 GCM.

The Regional Spectral Model (RSM) was developed at the National Centers for Environmental Prediction (NCEP; Juang and Kanamitsu, 1994; Juang *et al*, 1997) to provide a physically consistent regional model for the NCEP global model. The RSM was further modified at the Experimental Climate Prediction Center (ECPC; Roads et al. 2003) at the Scripps Institution of Oceanography, University of California, San Diego. The version of the RSM and the regional climate simulations analyzed here were previously described by Han and Roads (2004).

The PNNL regional climate model was developed based on the Penn State/NCAR Mesoscale Model MM5 (Grell et al. 1994). Leung et al. (2003a) described the model configuration and results of a 20-year simulation driven by the NCEP reanalysis. The simulations analyzed here were driven by one PCM control simulation and an ensemble of three PCM simulations for the future climate following a business as usual scenario Leung et al. (2003b&2004) analyzed the hydrologic impacts of climate change in the Columbia River Basin, Sacramento-San Joaquin Basin, and the Georgia Basin/Puget Sound region based on the regional simulations. In this study, we analyzed only the ensemble mean of the three PCM and regional climate simulations for the future climate although differences are quite large among the ensemble members even when averaged over 2040-2060.

The Mesoscale Atmospheric Simulation (MAS) model is a limited-area atmospheric model written on a sigma coordinate (Soong and Kim 1996). Atmospheric-land surface interactions are computed by the Soil-Plant-Snow (SPS) model (Mahrt and Pan 1984; Kim and Ek 1995) that is interactively coupled with the MAS. The coupled MAS-SPS model was originally developed at the LLNL and is currently developed and used at UCLA for regional climate and extended range forecast studies. Earlier analyses of the regional climate change data used in this study were presented by Kim (2000), Kim et al. (2002) and Kim (2003). In addition, performance of the MAS model used for this study was evaluated by Kim and Lee (2003) in an 8-year hindcast study.

Institution	Regional Model	Land Surface Scheme	RCM resolution	RCM domain	Global Model	Present-climate CO_2 conc.	CO_2 increase
UCLA	MAS	SPS Kim and Ek (1995)	36 km	Western U.S.	HadCM2	340 ppm	1.6x
ECPC	RSM	OSU/NCEP Mahrt and Pan (1984)	60 km	Continental U.S.	PCM	~350 ppm	1.36x
Iowa St.	RegCM2	BATS ver 1e Dickinson et al. (1992)	52 km	Continental U.S.	HadCM2	340 ppm	1.8x
PNNL	PNNL/ MM5 Leung et al. 2003	OSU Chen and Dudhia (2001)	40 km	Western U.S.	PCM	340 ppm	1.41x

Table 1: Properties of simulations analyzed here.

The RegCM2 (Giorgi et al. 1993a, b) simulation performed by Iowa State computed precipitation using a simplified version (Giorgi and Shields 1999) of the Hsie et al. (1984) explicit moisture scheme and the Grell (1993) convection parameterization. The model also used the BATS Version 1e (Dickinson et al. 1993) land surface model and the Holtslag et al. (1990) nonlocal boundary-layer turbulence parameterization. Radiative transfer used the CCM2 radiation package (Briegleb 1992). Pan et al. (2001) give further details of the simulation and discuss general features of the precipitation output and its change under greenhouse warming.

We evaluate these simulations by comparing them to a range of observational data products. In general these are gridded (i.e. spatially complete) data products that have been produced by applying physically-based spatial interpolation methods to sparse

observations. The exception is near-surface temperature data from the Global Historical Climatology Network (GHCN), whose station data we display after averaging onto a 0.5 deg grid. The value we show in each 0.5 deg box is the mean of all stations within that box; if there are no stations in the box that value is missing. Thus, no interpolation was performed on this data. Table 2 lists salient properties of the observational data sets used in this study.

Dataset source	Quantities used	Spatial resolution	Time resolution	Reference
VEMAP	T, P	0.5 deg.	monthly	http://www.cgd.ucar.edu/vemap/mainpage.html
NOAA	P	0.25 deg	daily	http://www.cdc.noaa.gov/PublicData/
GHCN	T			
NOHRSC	SWE			http://www.nohrsc.nws.gov/
UW	T	0.125 deg	monthly	http://www.hydro.washington.edu/Lettenmaier/gridded_data/index.html

Table 2: Observational data sets used for model evaluation. "Quantities used" lists meteorological quantities that were used in this study; additional quantities may be available from the same data source. T = near-surface temperature; P = precipitation; SWE = snow water equivalent (i.e., water-equivalent snow depth). VEMAP = Vegetation/Ecosystem Modeling and Analysis Project; NOAA = National Oceanic and Atmospheric Administration; GHCN = Global Historical Climatology Network. NOHRSC = National Operational Hydrologic Remote Sensing Center; UW = University of Washington.

3. Results

3.1 Present climate: Seasonal Means

We start by analyzing the ability of the four RCM/GCM simulations to reproduce aspects of the present climate in the western U.S. All four simulations overestimate spatially-averaged monthly-mean wintertime precipitation, in some months by as much as a factor of two (Figure 1). This figure also suggests that these biases in the RCM results are due to similar biases in the driving GCMs. (I.e., the RCMs produce too much precipitation because too much moisture enters their domains from the GCM.) However, the ECPC model (for example) over-predicts western U.S. precipitation when forced with lateral boundary conditions from reanalysis (Han and Roads, 2004)), as does RegCM2 (Pan et al., 2001; Gutowski et al. 2004); thus the tendency to overpredict western U.S. precipitation may be to some extent inherent in the RCMs. Although the different control simulations have similar spatially-averaged precipitation amounts, the different RCMs differ in how they spatially distribute wintertime precipitation (Figure 2). The too-wet bias is also apparent in Figure 2. Of the four control simulations, the HadCM2/MAS (UCLA) simulation has the most extreme spatial variations in wintertime precipitation; it is also the only control simulation in which Nevada and eastern Oregon are not much too wet.

The impressions gained from Figure 2 are quantified in Figure 3a, a "Taylor diagram" (Taylor, 2001) evaluating monthly-mean, spatially resolved precipitation in the RCMs and GCMs discussed here. This diagram compares simulated spatially-resolved quantities (in this case precipitation) to gridded observations (in this case VEMAP). Before these comparisons are made, the model results were interpolated to the grid of the observed data set (in this case 0.5 deg x 0.5 deg.). Caution must be taken that gridded observational data can be biased due to uneven distribution of stations. In particular a lack of high elevation stations in the western U.S. can cause systematic errors such as underestimation of spatial variability and warm biases in the near-surface air temperature (Kim and Lee 2003). Two statistics are shown, both based on climatological monthly-mean values at each location. The radial coordinate represents the standard deviation of model results divided by the standard deviation of observed values. This compares the magnitude of simulated spatio-temporal variability to observed variability; it confirms that for western U.S. precipitation the UCLA model has the most variability of all models considered, and more variability than observed precipitation. Figure 3a also shows that the RCMs have more spatio-temporal variability in simulated western U.S. precipitation than the GCMs do; it is typical for coarser-resolution models to have less variability. The angular coordinate in Figure 3 is the correlation coefficient between model results and observations; this measures the extent to which the maxima and minima in simulated quantities occur at the correct locations and times. Figure 3a shows that RCM-simulated precipitation correlates more strongly with observed precipitation than GCM-simulated precipitation does. In the Taylor diagram the results of an ideal model would be plotted on the horizontal axis at a radial coordinate value of 1; the distance on the plot from this

"ideal point" measures the RMS error in the model results. Thus, of all the models considered here, the PNNL model has the smallest RMS error in western U.S. precipitation. To give a feel for the importance of observational uncertainties, in Figure 3a we plot in the same manner as the models the NOAA observational data set.

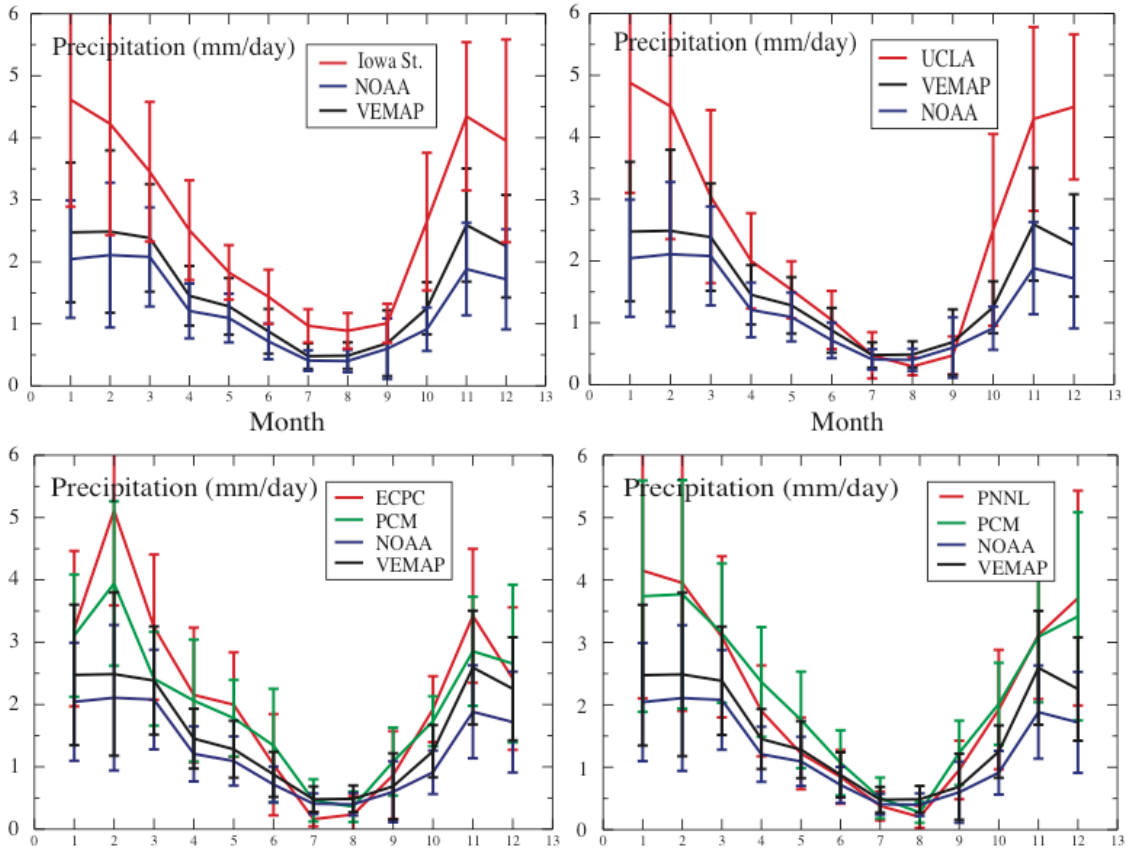

Figure 1: Seasonal cycle of present-day monthly-mean spatially-averaged precipitation in the western U.S. Each panel also shows results from one RCM. Next to the ECPC and PNNL RCM results are shown results from the PCM global simulations that provided lateral boundary conditions. Different PCM simulations were used to drive the two RCMS; thus the PCM results in the two lower panels are not identical. All panels show results of two observational data sets, from VEMAP and NOAA. Error bars represent interannual variability (1 std. deviation).

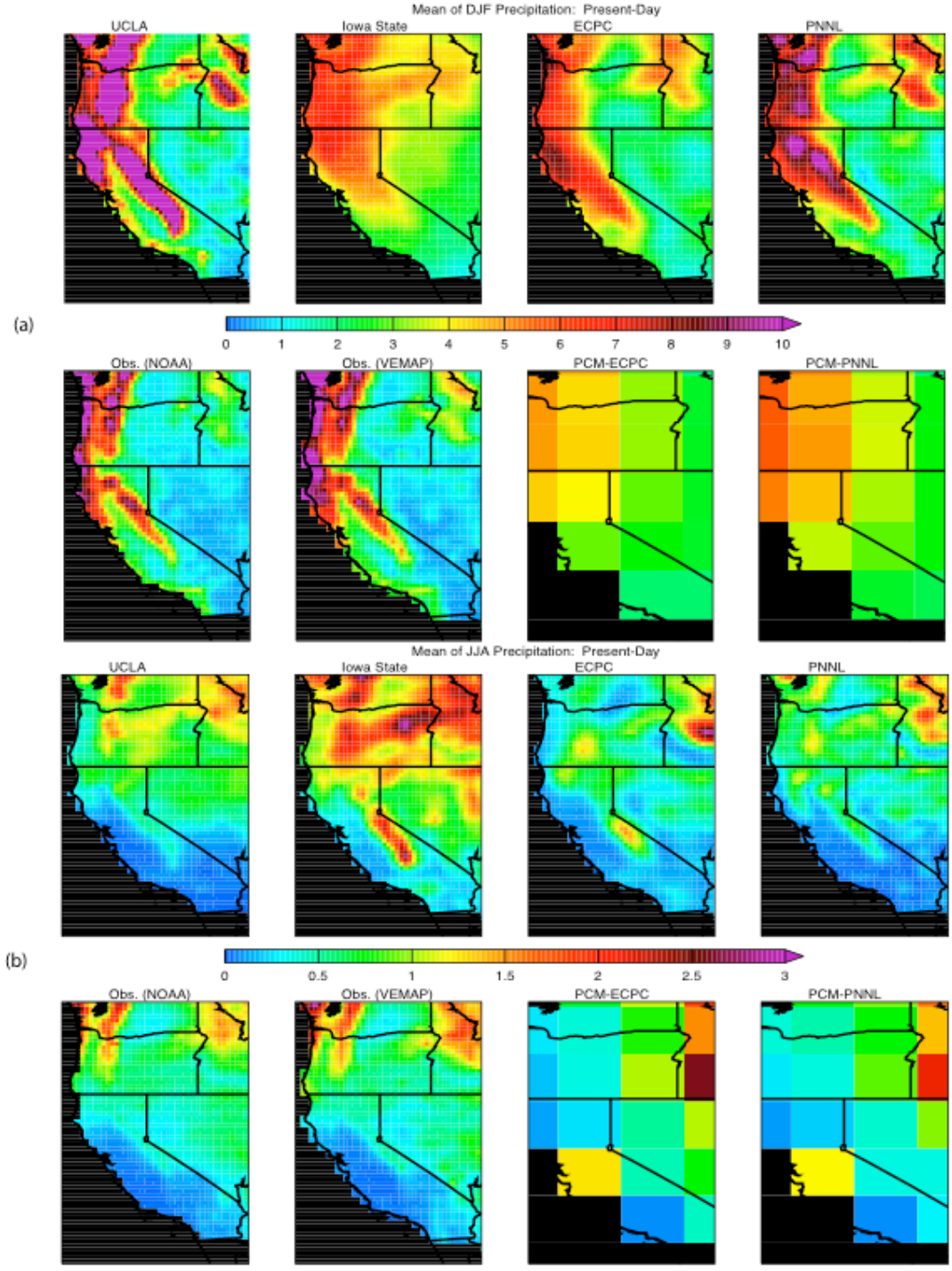

Figure 2: Maps of seasonal-mean precipitation in the western U.S. for (a) DJF and (b) JJA. In both (a) and (b) the top row shows results from four nested RCMs; the bottom row shows observed precipitation from NOAA and VEMAP (left) and results from two GCM simulations. Each GCM provided lateral boundary conditions to the RCM shown immediately above.

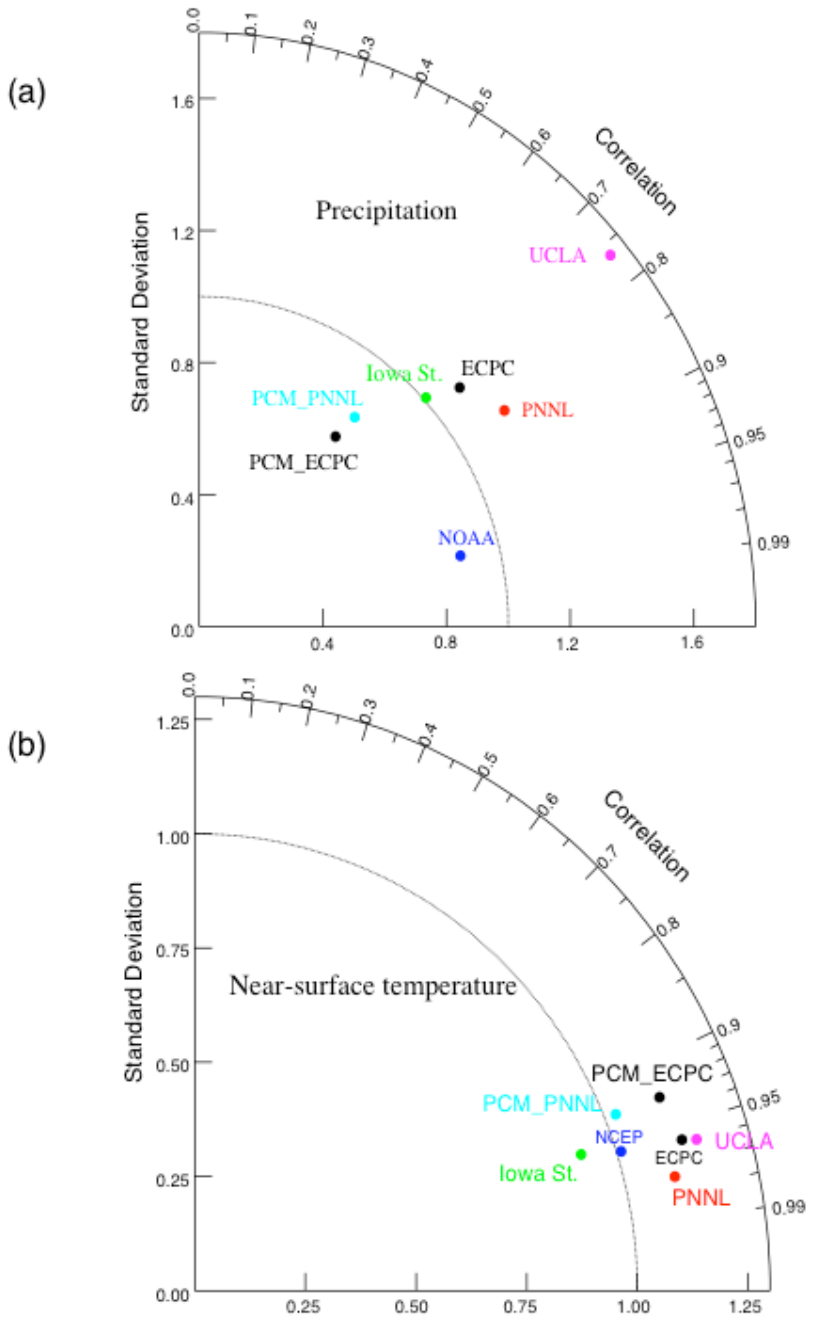

Figure 3: Taylor diagram evaluating simulations of precipitation (top) and near-surface temperature (bottom) in the Western U.S. The angular coordinate is the correlation coefficient between model results and observations (VEMAP). The radial coordinate is the standard deviation of model results divided by the standard deviation of observations. Before comparison to observations, model results were interpolated to the spatial grid of the observations. Statistics were calculated based on multi-year averages of monthly mean values at each geographical location. Results of a perfect model would be plotted on the horizontal axis at a radial coordinate value of 1. NOAA observations of

precipitation and temperatures from NCEP reanalysis are plotted to indicate the size of observational uncertainties.

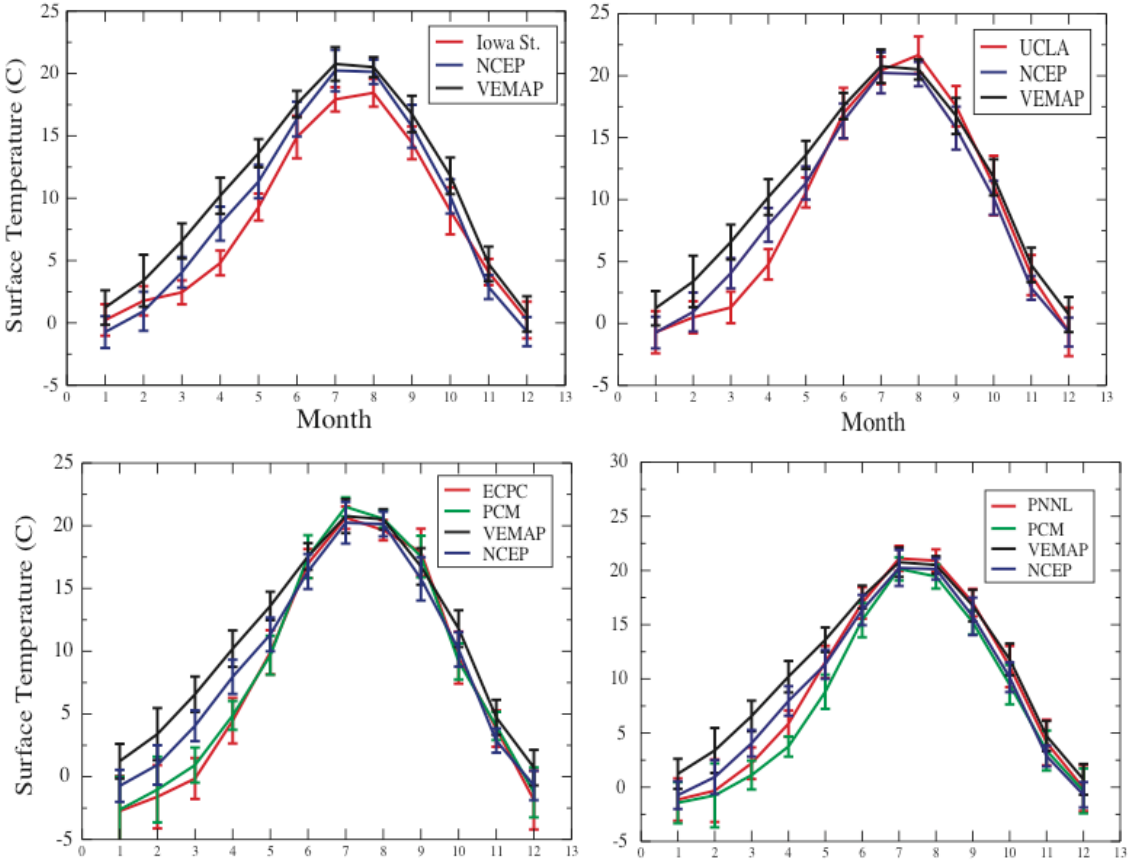

Figure 4: Seasonal cycle of present-day monthly-mean spatially-averaged near-surface temperature in the western U.S. Each panel also shows results from one RCM. Next to the ECPC and PNNL RCM results are shown results from the PCM global simulations that provided lateral boundary conditions. All panels show results of two observationally-derived data sets, from VEMAP and NCEP reanalysis. Error bars represent interannual variability (1 std. deviation).

The RCM/GCM control climates also show some significant biases in spatially-averaged monthly-mean near-surface temperatures (Figure 4). All the control climates are too cold in late winter and spring; the HadCm2/RegCM2 (Iowa State) simulation is also too cold in summer. These biases in the ECPC and PNNL results seem to result from similar biases in the driving PCM simulation. Maps of annually-averaged near-surface temperatures (Figure 5) show that all the RCMs simulate the basic spatial pattern of near-

surface temperature quite well; this is not surprising as this pattern is strongly determined by topographic variations. As with precipitation, the UCLA model shows the most spatial variability of the four RCMs in near-surface temperatures. This likely results at least in part from the higher spatial resolution used in this model compared to the other RCMs, which allows more accurate representation of topography.

A Taylor diagram (Figure 3b) shows that simulated near-surface temperatures correlate much more strongly with observed values than simulated precipitation does. As with precipitation, the UCLA results have the most spatio-temporal variability of all the simulations considered here. Figure 3b also shows that three of the RCMs have higher correlation coefficients (relative to the VEMAP data) in near-surface temperatures than the NCEP reanalysis does. One of these models has a smaller RMS error in near-surface temperature than NCEP does. This no doubt results from the relatively coarse spatial resolution of the reanalysis, which makes it unable to capture topographically-induced variations in near-surface temperatures.

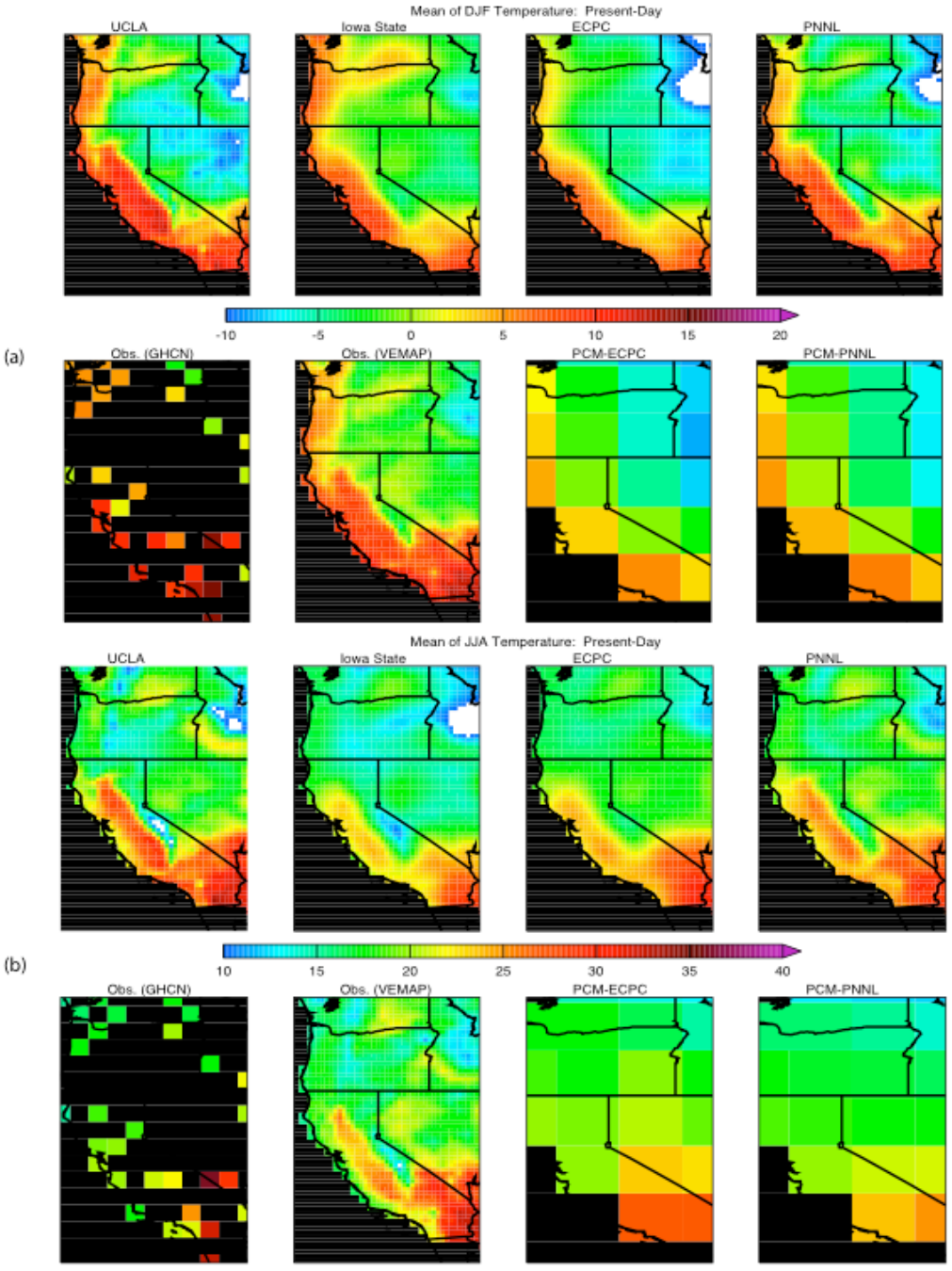

Figure 5: Maps of seasonal-mean near-surface air temperature in the western U.S. for (a) DJF and (b) JJA. In both (a) and (b) the top row shows results from four nested RCMs; the bottom row shows observed near-surface temperature from GHCN and VEMAP (left), as well as results from two GCM simulations that provided lateral boundary conditions to the RCM shown immediately above. For this comparison the GHCN (Global Historical Climatology Network) station data were averaged onto a 0.5 degree latitude/longitude grid; grid locations with no station data are black.

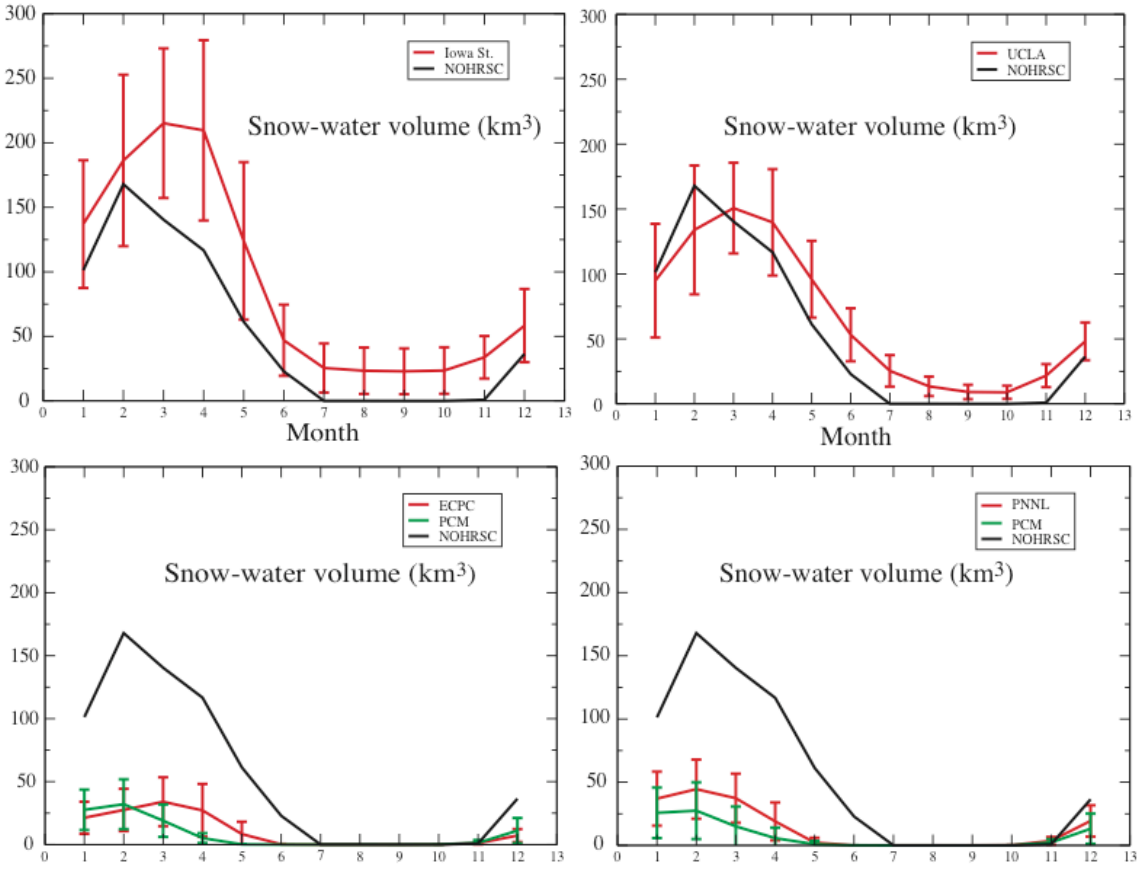

Figure 6: Seasonal cycle of present-day monthly-mean spatially-averaged water-equivalent snow volume in the western U.S. Each panel also shows results from one RCM, as well as from the NOHRSC assimilation data set. Error bars represent interannual variability (1 std. deviation). The NOHRSC snow dataset is an assimilation based on the model-forecasted precipitation and a snow model, and may not have the same accuracy as observed values.

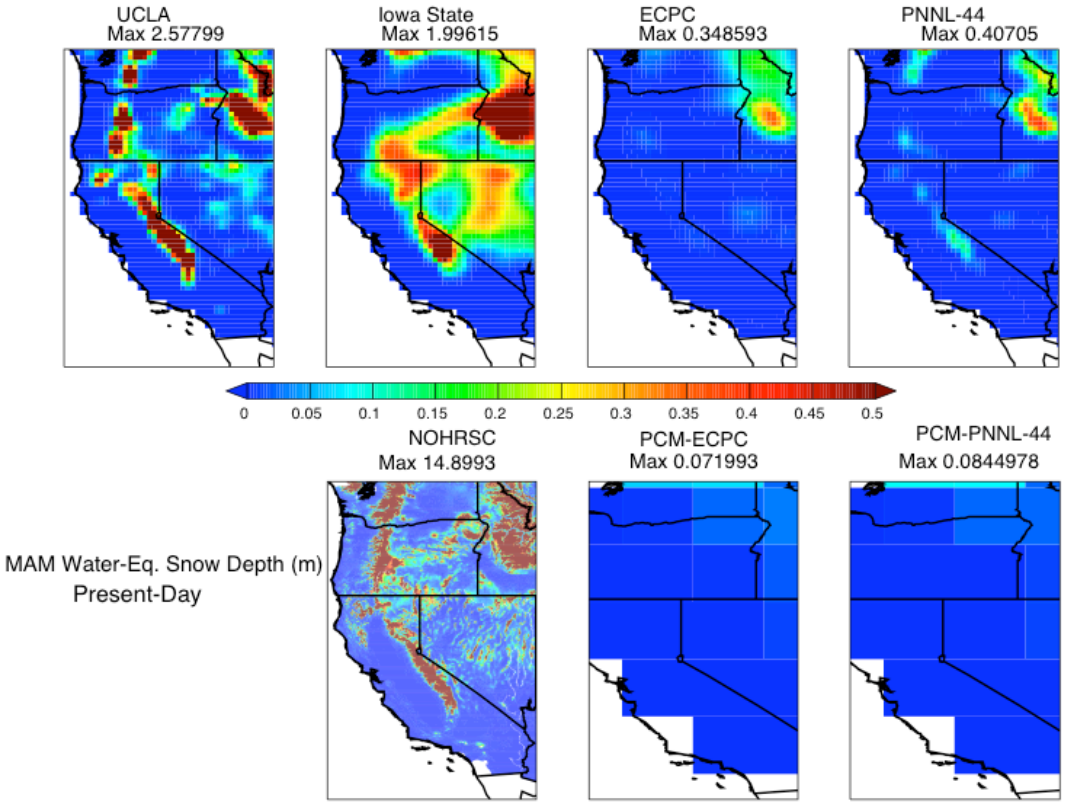

Figure 7: Maps of present-climate western U.S. water-equivalent snow depth, or snow-water equivalent (SWE) for March-April-May. The top row shows results from four nested RCMs. The bottom row shows observed values (left) and values from two GCM simulations that provided lateral boundary conditions to two of the RCMs.

Compared to data from NOHRSC, the PCM/RSM (ECPC) and PCM/MM5 (PNNL) simulations severely underestimate water-equivalent snow depths, or snow-water equivalent (SWE), in the western U.S. in every month except those in which there is no observed snow (Figure 6). The other control simulations overestimate SWE in spring, summer, autumn, and early winter. Maps of seasonal-mean SWE for MAM (Figure 7) confirm the biases seen in the spatially-averaged SWE results. In addition, Figure 7 shows some significant apparent errors in the simulated spatial distributions of SWE. For

example, the Iowa State model predicts too much SWE in Nevada and Eastern Oregon, and too little SWE in the Cascade Mountains of Oregon and Washington.

The snow amounts seen in the ECPC and PNNL control simulations appear to be inconsistent with those simulations' biases in monthly-averaged near-surface temperature and precipitation. Specifically, although these simulation under-predict SWE relative to NOHRSC in every month when snow is observed, both these simulations overestimate regionally-averaged precipitation throughout the rainy season (Figure 1), and underestimate regionally-averaged near-surface temperatures from January onwards (Figure 4). This suggests that these simulations should overestimate SWE, the opposite of what we find.

To try to explain this puzzle, in Figure 8 we show scatter plots of monthly-mean near-surface temperature biases versus monthly-mean precipitation biases. Here, the bias at each location is defined to be the difference between monthly-mean model result and climatological monthly-mean observed value from VEMAP. To confine the analysis to locations where snow is on the ground, we show results only for November through March, and only at locations where the observed NOHRSC SWE exceeds zero. (We interpolated all results to the VEMAP grid for this analysis; thus each point on the plot therefore corresponds to a 0.5 deg. x 0.5 deg. grid cell.) All the control simulations are predominately biased towards being too cold and wet, which should lead to too much SWE. For example, the median bias in near-surface temperature is -3.24 C in the ECPC simulation and -1.70 C in the PNNL simulation; median precipitation biases are 1.00

mm/day and 0.79 mm/day, respectively. Thus, in most locations where snow cover is observed, these simulations are too cold and too wet. In some locations the temperature biases in the RCM results exceed 15 C. The same scatter-plot analysis using an alternative near-surface data temperature set obtained from the Surface Water Modeling group at the University of Washington (http://www.hydro.washington.edu/Lettenmaier/gridded_data/), the development of which is described by Maurer et al. (2002), gave very similar results (not shown).

Thus, it is not clear from the meteorology shown in Figures 1, 4, and 8 why the UCSC and PNNL control simulations should underestimate snow amounts. One possibility is that snow amounts may increase nonlinearly with surface elevation; if this is the case, then in simulations such as those analyzed here where topography is under-resolved, one would expect SWE to be underestimated. Another possibility involves daily-timescale temperature and precipitation errors in these simulations. Specifically, our findings could result from positive temperature errors on days with large precipitation amounts (i.e. if the models are too warm during strong precipitation events). This has been seen in some regions of the western U.S. in other simulations with the PNNL model (Leung *et al.* 2003). Without access to daily temperature and precipitation results, however, we cannot determine if this is occurring in these RCM simulations.

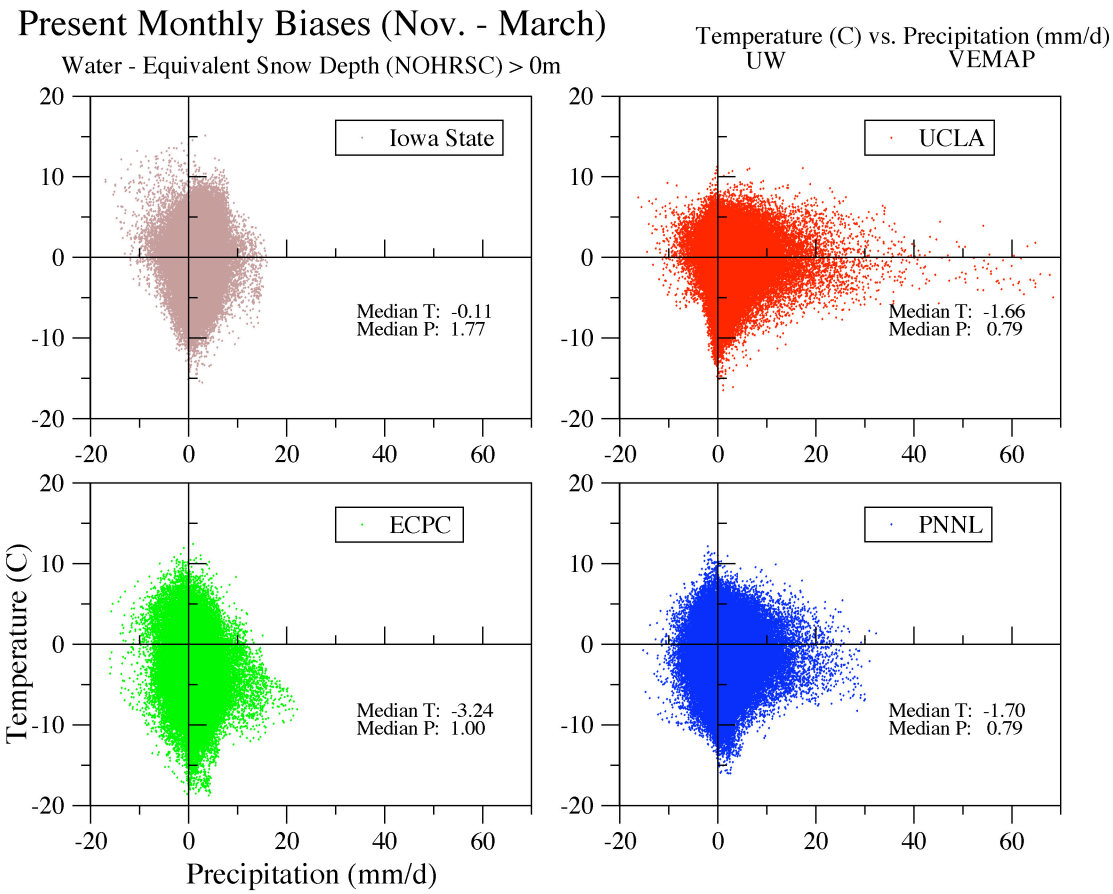

Figure 8: Scatter plots of model temperature biases versus precipitation biases. Here biases are calculated by subtracting climatological monthly-mean observed values obtained from VEMAP from monthly-mean model results. For this comparison the model results were interpolated to the grid of the observations (0.5 deg. x 0.5 deg.), thus each point corresponds to a half-degree grid cell. Only points where the observed snow cover exceeds zero are shown.

Defects in representations of land-surface processes can also cause large snow-accumulation biases. Leung and Qian (2003) analyzed regional climate simulations driven by the NCEP reanalysis for the western U.S. and found a large negative bias in snowpack. Their analysis suggested that up to 50% of the snowpack bias was related to temperature and precipitation bias, but deficiency in the land surface model likely accounted for a substantial part of the remaining bias. Similar results were seen in a recent intercomparison in which twenty-one land-surface models were forced with

observed meteorology for 18-year simulations (Slater *et al.*, 2001). Since snowfall was prescribed in these simulations, all intermodel differences in SWE, and, in principle, any model biases in SWE, result from inadequacies in the land-surface models. This intercomparison revealed large (up to factor of ~4) intermodel scatter in simulated SWE. The models' biases relative to observed SWE were predominately positive in some years and negative in others. It was also found that early-season biases tended to persist throughout the snow year. Further suspicion of defects in land surface models being a major source of model bias is the fact that both the RSM and PNNL model used a land surface model based on the OSU model with a single layer of snow. Clearly, the sorts of defects in land-surface models could be an important factor in SWE biases in the RCMs considered here.

Finally, the apparent inconsistency between the ECPC and PNNL RCMs' biases in near-surface temperature and precipitation and their biases in SWE could result at least in part from the limited number of years represented in the NOHRSC snow data. Specifically, this data set represents only 1996-2000, which may have more snow than normal in part because of the strong El Nino in 1997-1998. A snow data set including more years might result in smaller apparent model biases.

3.2: Present Climate: Interannual Variability

Interannual variations in climate in the western U.S. have important societal impacts. Variations in precipitation can be particularly important, resulting in stress on water

infrastructure, floods and mudslides. The primary source of interannual variability in this region is the El Nino/Southern Oscillation (ENSO), which introduces variability primarily on times scales of 4 to 7 years.

The control climates overestimate interannual variability of monthly-mean, regionally-averaged precipitation in nearly every month (Figure 9). This is perhaps to be expected given that the monthly mean precipitation is also too high in all the RCMs. The RCM errors in both mean precipitation and interannual variability of monthly-mean precipitation are largest in the winter months, when precipitation is also largest. All the simulations successfully represent the higher interannual variability in February relative to January and March. In January and February, the two PCM simulations differ greatly from each other in interannual variability of precipitation; however, each RCM nonetheless seems to closely follow its driving GCM.

Observations show relatively little seasonal cycle in interannual variability of monthly-mean, regionally-averaged near-surface temperatures (Figure 9). The PCM model and the RCMs driven by PCM, however, show more variability in winter than in summer and more variability than is observed in winter. The two RCMs that were driven by HadCM2 (Iowa State and UCLA) do better at estimating winter-time variability in time-and space-averaged near-surface temperatures.

Maps of interannual variability of seasonal-mean precipitation (Figure 10) show that locations of high interannual variability generally coincide with locations of high

seasonal-mean precipitation (Figure 2). The RCMs generally reproduce the observed spatial pattern of high interannual variability over mountains in California, Oregon, and Washington, and low variability over the dry regions in Eastern Oregon, Eastern Washington, and Nevada. The Iowa State model, however, has not enough variability in the mountains and too much in the dry regions. The ECPC model does not reproduce the observed high variability over the mountains in Washington and Oregon.

Maps of interannual variability of seasonal-mean near-surface temperature (Figure 11) show that the excessive variability seen in the ECPC model's spatially-averaged temperatures (Figure 9b) is due primarily to excessive variability inland (in eastern Oregon and Washington, Idaho, and northern Nevada). This clearly results from excessive variability in the same locations in the driving PCM simulation.

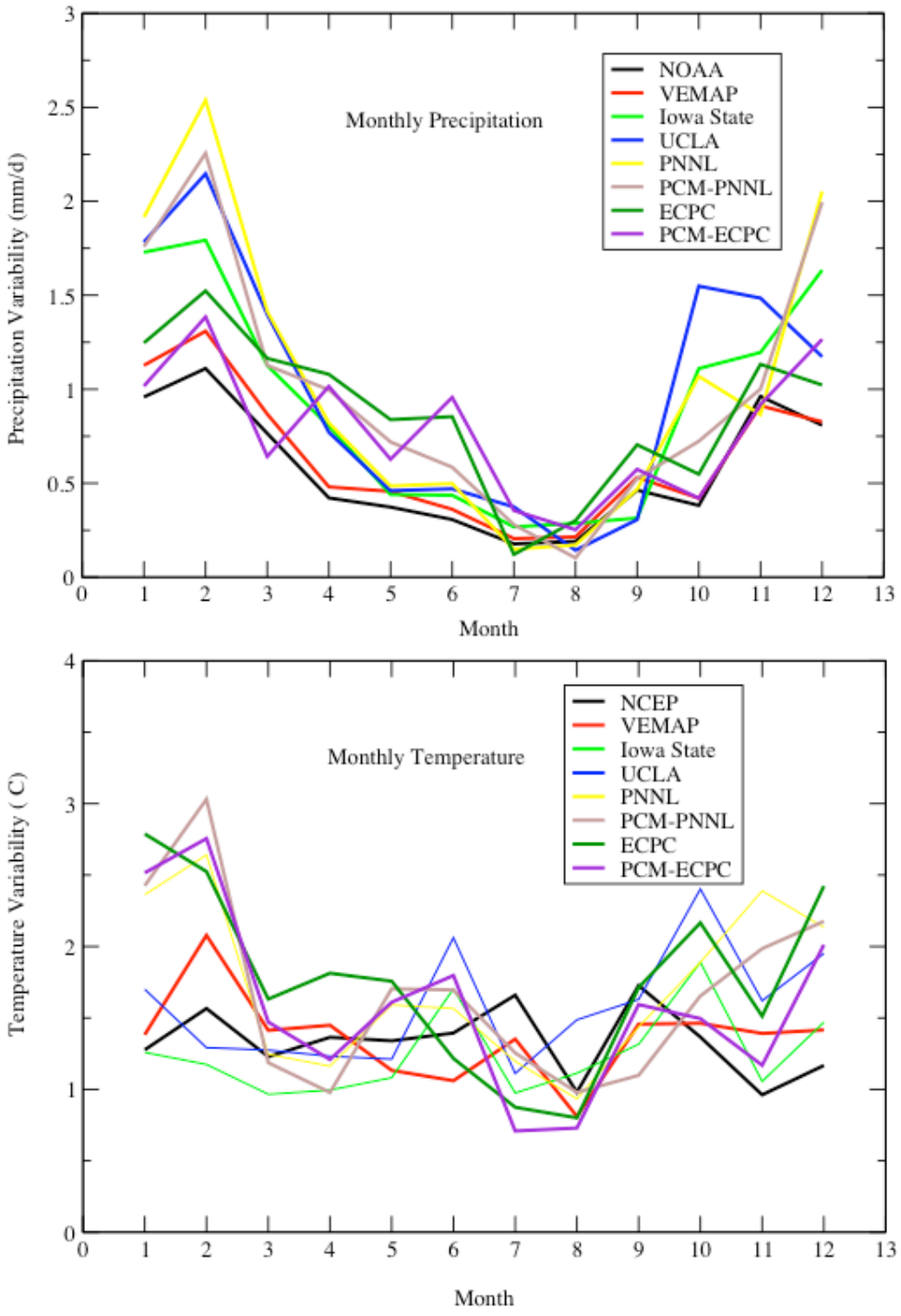

Figure 9: Internnual variability of monthly-mean, spatially-averaged precipitation (top) and near-surface temperature (bottom). For each month, the standard deviation (over years) of monthly-mean precipitation averaged over the study area is shown.

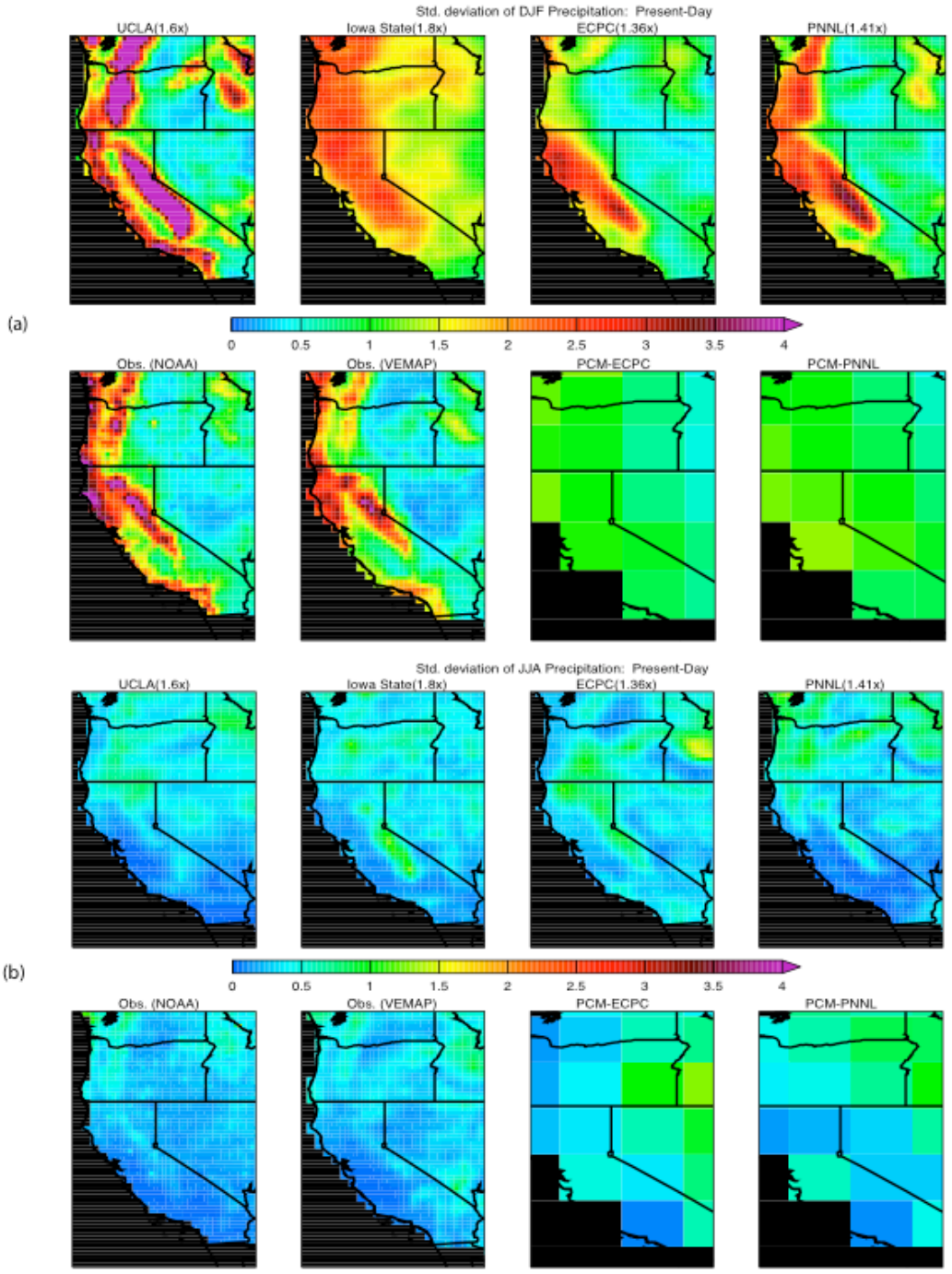

Figure 10: Interannual variability in seasonal-mean precipitation for (a) DJF and (b) JJA. In both (a) and (b), top row shows results from four RCMs. Bottom row shows results from two observational data sets (NOAA and VEMAP) as well as from two GCM simulations. Each GCM simulation provided boundary conditions to the RCM shown immediately above it. Here, interannual variability is represented by the standard deviation of results from 10 years of observations or simulations.

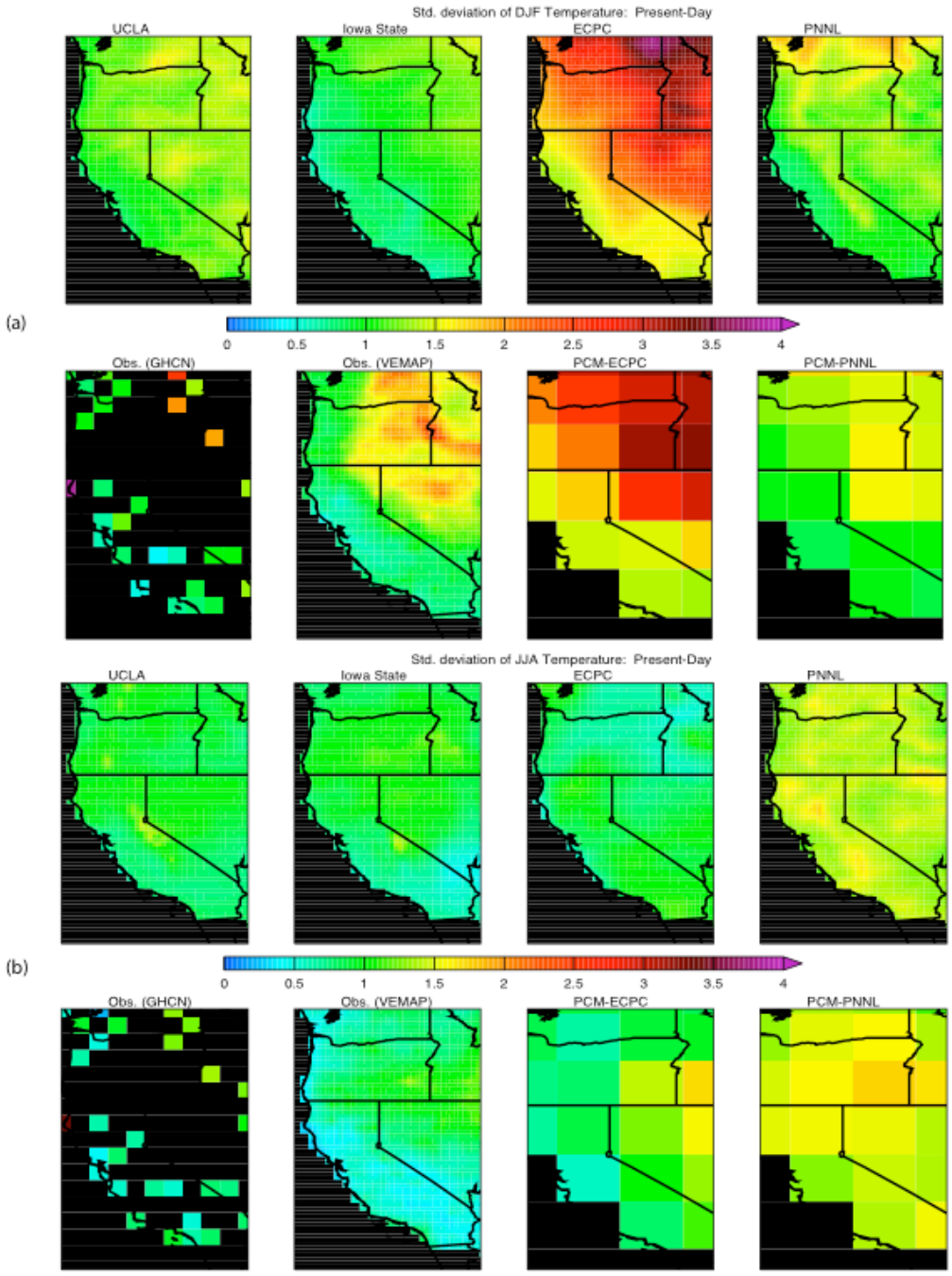

Figure 11: Interannual variability in seasonal-mean near-surface temperature for (a) DJF and (b) JJA. In both (a) and (b), top row shows results from four RCMs. Bottom row shows results from two observational data sets (GHCN and VEMAP) as well as from two GCM simulations. Each GCM simulation provided boundary conditions to the RCM shown immediately above it. Here, interannual variability is represented by the standard deviation of results from 10 years of observations or simulations.

3.3 Simulated responses to increased greenhouse gases

We start by examining the simulated response of regional precipitation to increased CO_2. In the two RCMs driven by results from the PCM global model, the regionally-averaged monthly-mean response is consistent with zero in every month (Figure 12). This reflects a similarly insignificant regional precipitation response in the PCM results. Especially in the PNNL results, it is striking how closely the RCM response follows that of PCM; this similarity includes not only the multi-year average response, but also the magnitude of interannual variability (indicated by error bars in Figure 12). The lack of a significant precipitation response in PCM and in the RCMs driven by PCM is consistent with the generally weak climate sensitivity of the PCM model to increased greenhouse gases (Barnett *et al.*, 2001), and with the relatively small CO_2 increases considered in these simulations (1.36x and 1.41x).

To avoid confusing a response to increased CO_2 with interannual variability, we assessed the statistical significance of simulated precipitation responses relative to interannual variability at each model grid cell. This was done using a 2-sided student's t-test. The RCM simulations driven by results from PCM show almost no area where the simulated precipitation response is significant at a 90% or greater confidence level (Figure 13). This again may result from the relatively small CO_2 increases used in these simulations. The UCLA and Iowa State RCMs show statistically significant increases in precipitation in northern California, eastern Oregon, and central Idaho. The spatial pattern of simulated

precipitation response is quite similar in these two models, when only regions with statistically significant responses are considered.

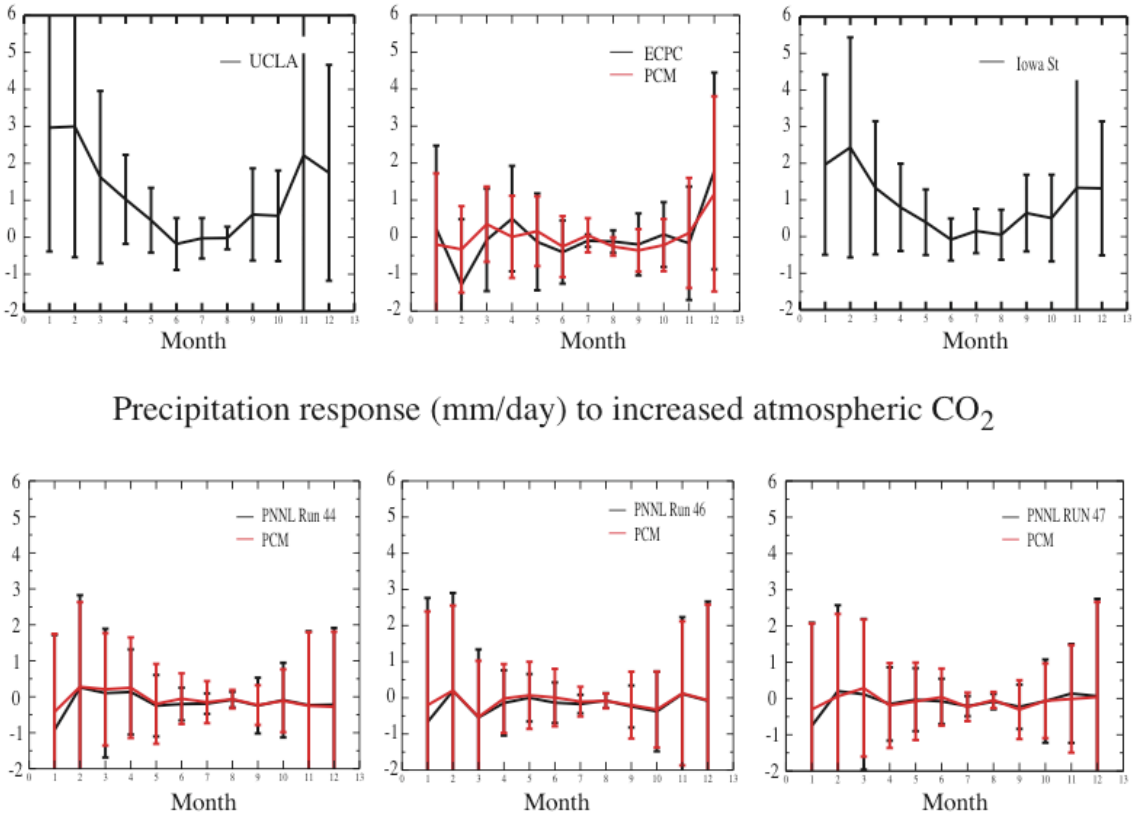

Figure 12: Seasonal cycle of monthly-mean spatially-averaged precipitation response to increased CO_2 in the western U.S. Each panel shows results from one RCM. Next to the ECPC and PNNL RCM results are shown results from the PCM global simulations that provided lateral boundary conditions. Error bars represent interannual variability (1 std. deviation).

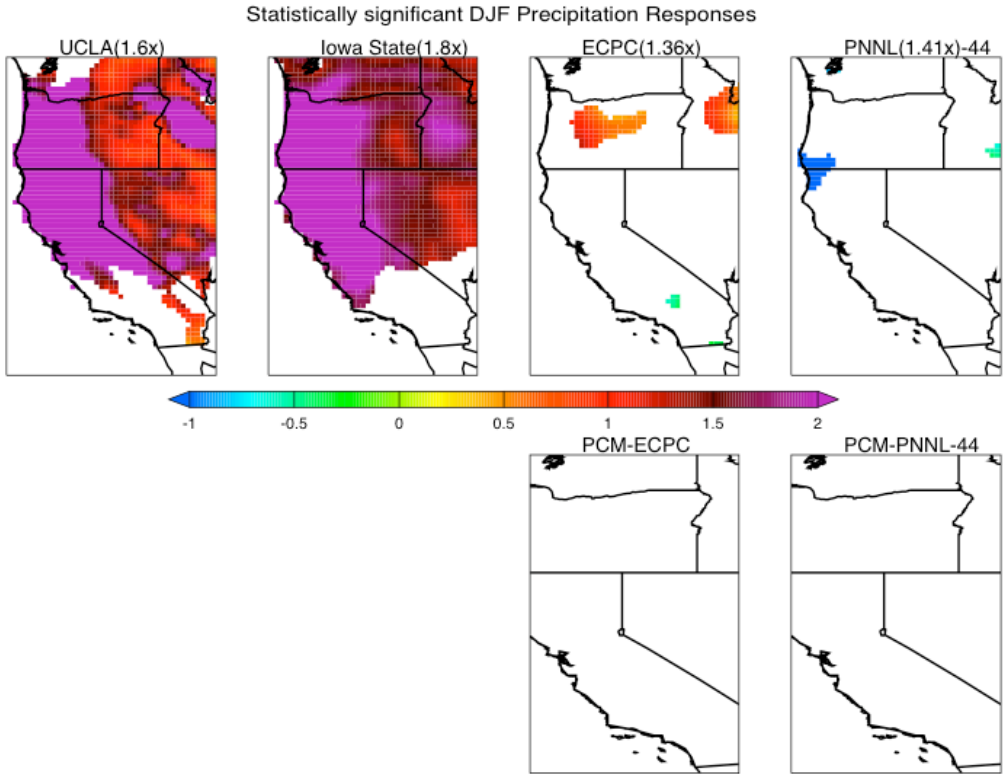

Figure 13: Maps of simulated response of wintertime (DJF) precipitation in the western U.S. to increased atmospheric CO_2. Units are mm/day. The top row shows results from four nested RCMs. The bottom row shows results from two GCM simulations that provided lateral boundary conditions to two of the RCMs. Results are shown only in areas where the precipitation response is significant relative to interannual variability at a 90% or greater confidence level; this is determined by applying a 2-sided student's t-test.

Simulated responses in near-surface temperatures to increased CO_2 show no significant seasonal cycle (Figure 14). As expected, the larger CO_2 increases in the UCLA and Iowa State simulations, combined with the larger climate sensitivity of HADCM2 than PCM, produce larger responses in near-surface temperatures. As with simulated precipitation responses, it is striking how closely the spatially averaged response in the ECPC and PNNL RCMs follows that in their respective driving GCM results. Maps of annual-mean

near-surface temperature responses (Figure 15) show that the UCLA and Iowa State models produce uniformly larger responses in near-surface temperatures.

To allow easier comparison of the spatial patterns of temperature responses across the various models, we show in Figure 16 normalized near-surface temperature responses. Here the simulated temperature response in each model has been multiplied by a scalar chosen so that the spatial mean of the normalized response is one. The RCMs agree that warming will be greater inland than near the coast, but they do not agree on details of the pattern of temperature response. The ECPC model has a notably different pattern of surface temperature response than the other models. This may be related to the lack of snowpack along the coastal mountains in the RSM control and future climate simulations, which precludes snow albedo feedback effects that play a role in the larger warming along the coastal mountains in all other RCM simulations.

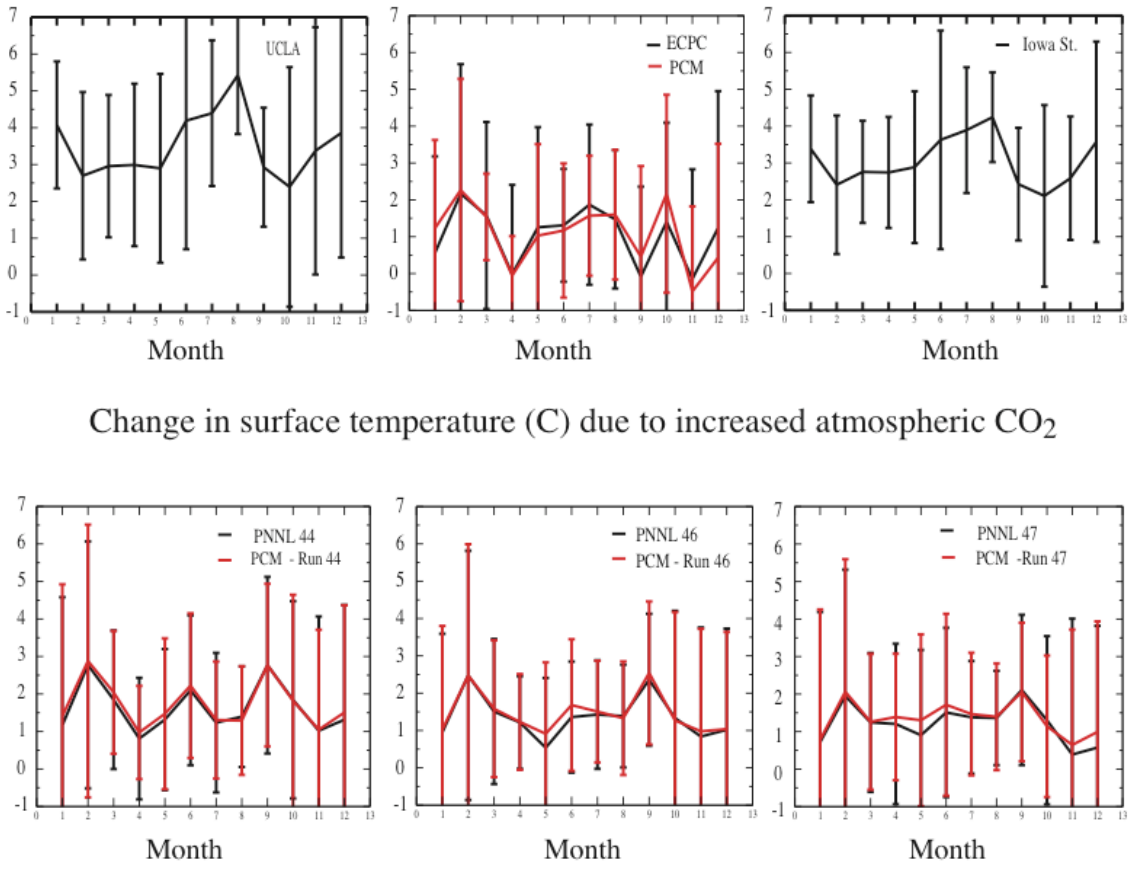

Figure 14: Seasonal cycle of monthly-mean spatially-averaged near-surface temperature response to increased CO_2 in the western U.S. Each panel also shows results from one RCM. Next to the ECPC and PNNL RCM results are shown results from the PCM global simulations that provided lateral boundary conditions. Error bars represent interannual variability (1 std. deviation).

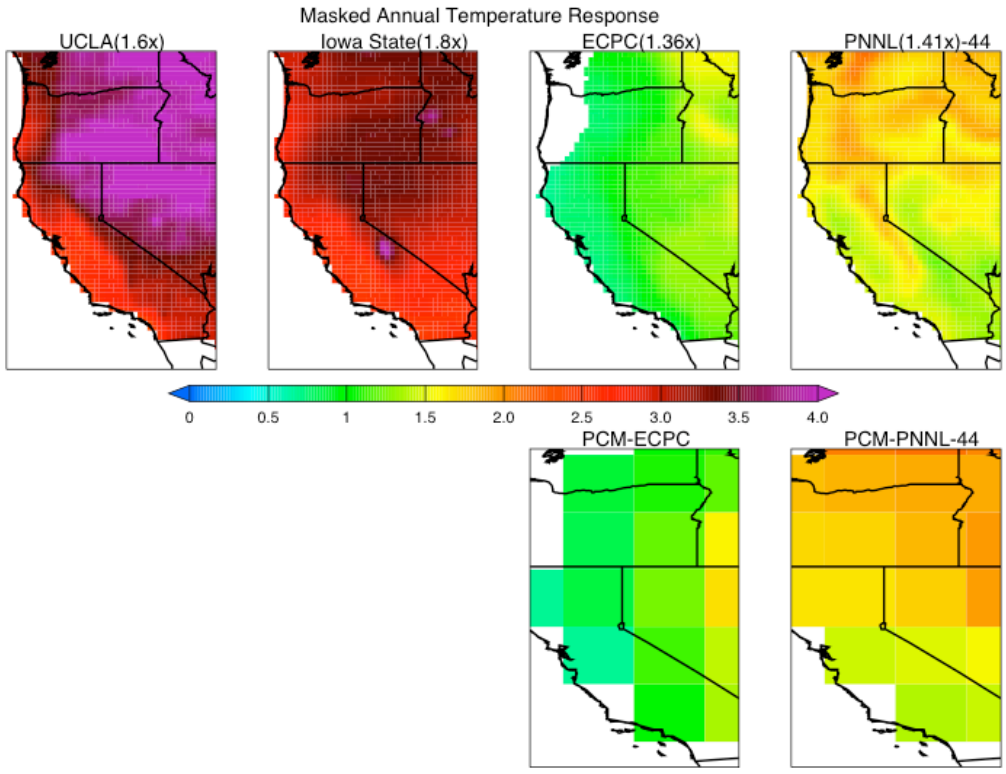

Figure 15: Maps of simulated response of annual-mean near-surface temperature in the western U.S. to increased atmospheric CO_2. The top row shows results from four nested RCMs. The bottom row shows results from two GCM simulations that provided lateral boundary conditions to two of the RCMs. Results are shown only in areas where the temperature response is significant relative to interannual variability at a 90% or greater confidence level; this is determined by applying a 2-sided student's t-test.

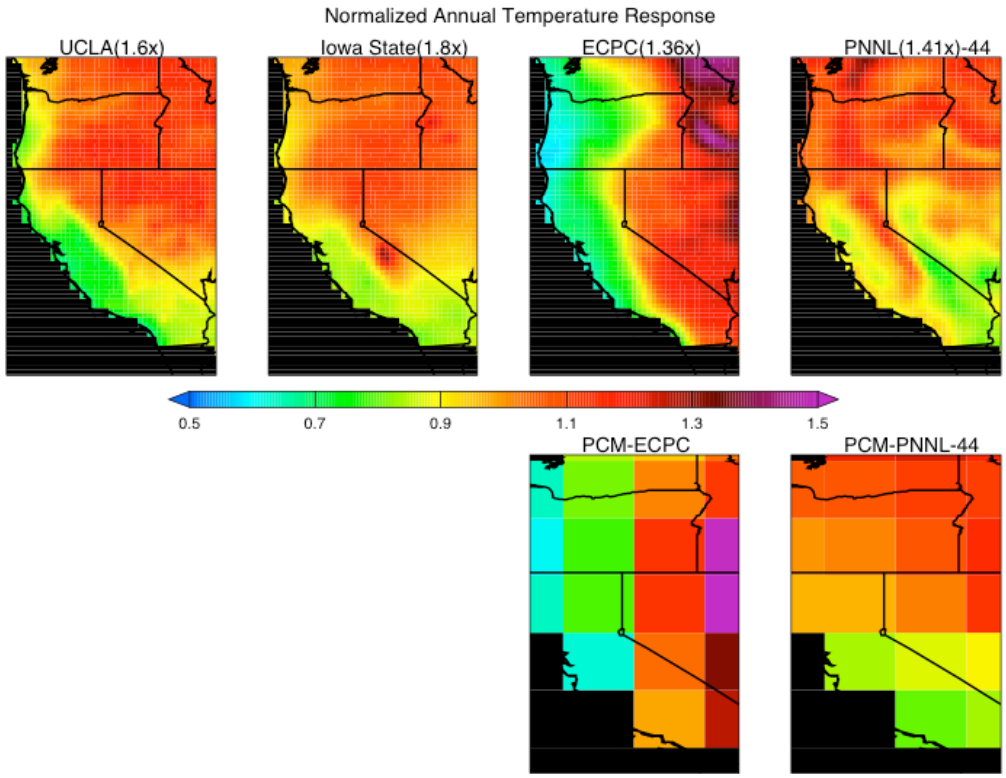

Figure 16: Maps of normalized response of annual-mean near-surface temperature in the western U.S. to increased atmospheric CO_2. Here, temperature response values have been normalized such that the spatial mean in each panel is 1. This allows the spatial patterns of temperature responses in the different models to be easily compared. The top row shows results from four nested RCMs. The bottom row shows results from two GCM simulations that provided lateral boundary conditions to two of the RCMs.

4. Discussion and conclusions

In order to incorporate climate change into planning processes, policymakers need projections of climate change that include quantitative estimates of uncertainties. One approach to producing such estimates is to compare results across a range of equally credible models. For uncertainty estimates to be quantitatively rigorous, a carefully-coordinated study in which all models consider the same climate change scenario, etc., is

needed. Such studies require a major, multi-institutional effort, however, and are beyond the scope of this paper. Here, we have instead compared available RCM simulations of the Western U.S., a region with diverse climates and clear vulnerabilities to climate change. This study may be viewed as one step toward the broader analysis that would involve carefully coordinated, multi-institutional simulations and cross-comparisons.

We analyzed the ability of the four RCM/GCM combinations to reproduce observations of the present climate, and the inter-model range of predicted responses to increased atmospheric greenhouse gases. In simulations of the present climate, the RCM results show significant biases; in most cases where driving GCM results are available, the RCM biases are very similar to the biases of the driving GCM within the RCM domain. Thus, the RCMs are doing an effective job of downscaling the GCM solutions. For example, the PNNL and ECPC models have positive precipitation biases in winter that are very similar to the biases in the driving PCM simulations. The UCLA and Iowa State models also have positive precipitation biases in winter. While we did not have access to the particular HadCM2 simulation used to drive the UCLA and Iowa State models, this bias is very similar to that seen in other HadCM2 simulations. Although the GCM simulations exert large control over the regional mean precipitation of the RCMs, the spatial distribution of precipitation can vary substantially among RCMs even when driven by the same GCM. These differences are likely dependent on model topography (with varying degrees of spatial smoothing typically applied) and model physics. All the RCMs analyzed here seem to have less SWE than one would expect from their biases in precipitation and near-surface temperature. In particular, the PNNL and ECPC models

have much less SWE than is observed, despite being too cold and having too much precipitation in most locations in our study area.

There is little consistency among the models as to responses in precipitation and near-surface temperatures to increased greenhouse gases. The two models driven by PCM (PNNL and ECPC) project no significant changes in regionally-averaged monthly-mean precipitation. Projected precipitation changes are not significant at the 90% confidence level in any location in the study area. This may be related to the small CO_2 increases (1.41x and 1.36x, respectively) in these simulations. The two RCMs driven by HadCM2 (UCLA and Iowa State) predict increases in monthly-mean regionally-averaged wintertime precipitation that are comparable in magnitude to the interannual variability of the precipitation response (one standard deviation); i.e., are barely significant. These RCMs predict precipitation increases that are significant at the 90% confidence in northern California, eastern Oregon, and central Idaho. All the RCMs predict warming in response to increased greenhouse gases. The models that simulated larger CO_2 increases and were driven by GCMs with larger climate sensitivity (UCLA and Iowa State) predict greater warming. There is no significant seasonal cycle to the predicted warming in any RCM, and the spatial patterns of predicted warming are quite different in the different RCMs.

Acknowledgements

This work was performed under the auspices of the U.S. Department of Energy by the Lawrence Livermore National Laboratory under contract No. W-7405-Eng-48. The ECPC RSM work was supported in part by NOAA NA17RJ1231.

References

Anderson, C.J., R. W. Arritt, E. S. Takle, Z. Pan, W. J. Gutowski, R. da Silva, and PIRCS modelers, 2003: Hydrologic processes in regional climate model simulations of the central United States flood of June-July 1993. *J. Hydrometeor, 4*, 584-598.

Barnett, T.P., D.W. Pierce, and R. Schnur, 2001: Detection of anthropogenic climate change in the world's oceans. *Science*, 292, 270-274.

CCSI, cited as 2004: www.cics.uvic.ca/scenarios/index.cgi.

Chen, F. and J. Dudhia, 2001: Coupling an advanced land surface-hydrology model with the Penn State-NCAR MM5 modeling system Part 1: Model implementation and sensitivity. *Mon. Wea. Rev. 129*, 569-585.

Christensen, J.H., T. Carter, F. Giorgi: PRUDENCE Employs New Methods to Assess European Climate Change, EOS, *82*, p. 147, 2002.

Coquard, J., P. B. Duffy, and K. E. Taylor, 2004: Present and future surface climate in the Western U.S. as simulated by 15 global climate models, accepted by *Climate Dynamics*.

Dickinson, R.E., A. Henderson-Sellers, and P.J. Kennedy, 1992: Biosphere-atmosphere transfer scheme (BATS) version 1e as coupled to NCAR community climate model, *NCAR Tech. Note 387+STR*, 72pp, Nat'l Cent. for Atmos. Res., Boulder Co.

Gutowski, W. J., F. Otieno, R. W. Arritt, E. S. Takle and Z. Pan, 2004: Diagnosis and attribution of a seasonal precipitation deficit in a U.S. regional climate simulation. *J. Hydrometeor,* 5**,** 230-242.

Han, J., and J. Roads, 2004: US Climate Sensitivity Simulated with the NCEP Regional Spectral Model. *Climate Change*, 62, 115-154, doi:10.1023/B:CLIM.0000013675.66917.15

Juang, H.-M. H, S.-Y. Hong, and M. Kanamitsu, 1997: The NCEP Regional Spectral Model: an update, *Bull. Amer. Meteorol. Soc., 78*, 2125-2143.

Juang, H.-M. H, and M. Kanamitsu, 1994: The NMC nested Regional Spectral Model, *Mon. Wea. Rev., 122*, 3-26.

Kim, J., 2001: A nested modeling study of elevation-dependent climate change signals in California induced by increased atmospheric CO_2. *Geophys. Res. Lett., 28*, 2951-2954.

Kim, J., T. Kim, R. W. Arritt, and N. L. Miller, 2002: Impacts of increased atmospheric CO_2 on the hdyroclimate of the western United States. *J. Climate, 15*, 1926-1942.

Kim, J. and J. Lee, 2003: A multiyear regional climate hindcast for the western United States using the Mesoscale Atmospheric Simulation model. *J. Hydrometeorol*, *4*, 878-890.

Kim, J., 2003: A projection of the effects of the climate change induced by increased CO_2 on extreme hydrologic events in the western U.S., submitted to *Climatic Change*.

Leung, L.R., Y. Qian, and X. Bian, 2003: Hydroclimate of the western United States based on observations and regional climate simulation of 1981-2000. Part I: Seasonal statistics. *J. Clim.*, 16(12), 1892-1911.

Leung, L.R., and Y. Qian, 2003: Changes in seasonal and extreme hydrologic conditions of the Georgia Basin/Puget Sound in an ensemble regional climate simulation for the did-century. *Canadian Water Resources Journal*, Vol. 28, No. 4, 605-631.

Leung, L.R., and Y. Qian, 2003: The sensitivity of precipitation and snowpack simulations to model resolution via nesting in regions of complex terrain. *J. Hydrometeorol.*, 4, 1025-1043.

Leung, L.R., Y. Qian, X. Bian, W.M. Washington, J. Han, and J.O. Roads, 2004: Mid-century ensemble regional climate change scenarios for the western United States, *Climatic Change*, 62(1-3), 75-113.

Mahrt, L. and H.-L. Pan, 1984: A two-layer model of soil hydrology, *Bound-layer Met., 29*, 1-20.

Maurer, E.P., A.W. Wood, J.C. Adam, D.P. Lettenmaier, and B. Nijssen, 2002, A Long-Term Hydrologically-Based Data Set of Land Surface Fluxes and States for the Conterminous United States, *J. Climate 15,* 3237-3251.

NOHRSC: National Operational Hydrologic Remote Sensing Center. http;//www.nohrsc.nws.gov/.

Pan, Z., J. H. Christensen, R.W. Arritt, W.J. Gutowski, Jr., E.S. Takle, and F. Otieno, 2001: Evaluation of uncertainties in regional climate change simulations. *J. Geophys. Res., 106,* 17,735-17,752.

RMIP, cited as 2003: http://www.start.org/project_pages/rcm.html.

Roads, J., S.-C. Chen, M. Kanamitsu, 2003: US Regional Climate Simulations and Seasonal Forecasts. *Journal of Geophysical Research-Atmospheres,* 108 (D16), 8606, doi:10.1029/2002JD002232.

Soong, S.-T. and J. Kim, 1996: Simulation of a heavy wintertime precipitation event in California, *Climatic Change, 32*, 55-77.

Slater, A.G., C. A. Schlosser, C. E. Desborough , A. J. Pitman, A. Henderson- Sellers , A. Robock , K. Ya. Vinnikov , K. Mitchell, A. Boone, H. Braden, F. Chen, P. Cox, P. de Rosnay, R.E. Dickinson, Y-J. Dai, Q. Duan, J. Entin, P. Etchevers, N. Gedney, Ye. M. Gusev, F. Habets, J.Kim, V. Koren, E.Kowalczyk, O.N.Nasonova, J.Noilhan, J. Shaake, A.B. Shmakin,T. Smirnova, D. Verseghy, P. Wetzel , Y. Xue, Z-L. Yang, 2001: The representation of snow in land-surface schemes: results from PILPS 2(d), *J. Hydrometeorology, 2*, pp. 7-25.

Takle, E. S., W. J. Gutowski, R. A. Arritt, Z. Pan, C. J. Anderson, R. R. da Silva, D. Caya, S.-C. Chen, J. H. Christensen, S.-Y. Hong, H.-M. H. Juang, J. Katzfey, W. M. Lapenta, R. Laprise, P. Lopez, J. McGregor and J. O. Roads, 1999: Project to Intercompare Regional Climate Simulations (PIRCS): Description and initial results. *J. Geophys. Res., 104,* 19,443-19,461.

Taylor K. E., 2001: Summarizing multiple aspects of model performance in a single diagram. *J. Geophys. Res., 106*, 7183-7192.